Published in final edited form as:
J Clin Neurosci. 2012 June ; 19(6): 875–880. doi:10.1016/j.jocn.2011.12.016.

A novel adenoviral vector labeled with superparamagnetic iron oxide nanoparticles for real-time tracking of viral delivery

Jonathan Yun[a], **Adam M. Sonabend**[a], **Ilya V. Ulasov**[c], **Dong-Hyun Kim**[d], **Elena A. Rozhkova**[e], **Valentyn Novosad**[d], **Stephen Dashnaw**[b], **Truman Brown**[b], **Peter Canoll**[a], **Jeffrey N. Bruce**[a], and **Maciej S. Lesniak**[c,*]

[a]Gabriele Bartoli Brain Tumor Laboratory, Columbia University Medical Center, New York, NY, USA

[b]Hatch Center for MRI Research, Columbia University Medical Center, New York, NY, USA

[c]Brain Tumor Center, Division of Neurosurgery, the University of Chicago, 5841 S. Maryland Avenue, MC 3026, Chicago, IL 60637, USA

[d]Argonne National Laboratory, Materials Science Division, Argonne, IL, USA

[e]Argonne National Laboratory, Center for Nanoscale Materials, Argonne, IL, USA

Abstract

In vivo tracking of gene therapy vectors challenges the investigation and improvement of biodistribution of these agents in the brain, a key feature for their targeting of infiltrative malignant gliomas. The glioma-targeting Ad5/3-cRGD gene therapy vector was covalently bound to super-paramagnetic iron oxide (Fe_3O_4) nanoparticles (SPION) to monitor its distribution by MRI. Transduction of labeled and unlabeled vectors was assessed on the U87 glioma cell line and normal human astrocytes (NHA), and was higher in U87 compared to NHA, but was similar between labeled and unlabeled virus. An *in vivo* study was performed by intracranial subcortical injection of labeled-Ad5/3-cRGD particles into a pig brain. The labeled vector appeared *in vivo* as a T2-weighted hyperintensity and a T2-gradient echo signal at the injection site, persisting up to 72 hours post-injection. We describe a glioma-targeting vector that is labeled with SPION, thereby allowing for MRI detection with no change in transduction capability.

Keywords

Adenovirus; Gene therapy; Nanoparticle

1. Introduction

The standards of therapy for glioblastoma reveal a need for novel treatment options.[1] Better understanding of the molecular pathogenesis of this disease in recent years has uncovered many potential targets,[2] increasing the promise of virus-mediated gene therapy. Adenoviruses are versatile vectors for gene therapy and are efficient carriers of large transgene constructs.[3–5] In a promising trial, an adenovirus vector was shown to reconstitute wild-type *p53* in malignant gliomas following intra-tumoral injection.[6]

[*]Corresponding author. Tel.: +1 (773) 834 4757; fax: +1 (773) 834 2608. mlesniak@surgery.bsd.uchicago.edu (M.S. Lesniak).

Disclosure/conflict of interest
The authors have no disclosures or conflict of interest for the work presented in this manuscript.

A limitation of wild-type adenovirus-based gene therapy is the low expression of the coxsackie-associated receptor (CAR) on the surface of glioma cells,[7–9] which limits tropism. We have described a novel adenovirus 5/3 chimera with the tripeptide arginine-glycine-aspartic acid (RGD) motif (Ad5/3-cRGD), which allows increased glioma-specific transduction by targeting CD46 and integrins.[10–17]

Malignant brain tumors infiltrate into the surrounding parenchyma, [18] and limited distribution of these vectors precludes successful tumor targeting. Strategies for improved delivery, such as convection-enhanced delivery,[19] may optimize vector distribution, but require the means for *in vivo* detection to be perfected. Although previous studies have attempted to measure the distribution of vectors with co-infusion of MRI-detectable agents,[20–22] the distribution of the vector and the detectable agent is not identical.

The utility of super-paramagnetic iron oxide (Fe_3O_4) nanoparticles (SPION) as an MRI contrast agent has been extensively studied. [23–26] Here, we use SPION-labeled Ad5/3-cRGD, providing specificity for MRI detection. Although nanoparticle-labeled adenoviruses have been studied,[27] no *in vivo* study of direct delivery in a large brain model has been attempted. We provide a proof of principle for the use of SPION-labeled viral vectors for assessment of their distribution in the brain.

2. Methods

2.1. Synthesis of SPION and labeled viral capsids

SPION (10 nm) were synthesized using the procedures of Sun et al., and using reagents from Sigma-Aldrich (St Louis, MO, USA).[28] The SPION were transferred to aqueous solution via the oleate and oleylamine ligand exchange reaction. A 10 mL hexane solution of 20 mg of SPION and 60 mg (0.36 mmoles) of 3,4-dihydroxyphenylacetic acid (DOPAC) in dichloromethane was mixed and stirred overnight. The mixture was centrifuged, dried, and washed with ethanol. The particles were re-dispersed in phosphate buffered saline (PBS). A solution of Fe_3O_4-DOPAC (10 mg) in 10 mmol PBS, pH 6.3, was mixed with 100 mg (0.1 mmoles) of sulfo-N-hydroxysuccinimide (NHS) and 20 mg (0.5 mmoles) of 1-ethyl-3-(3-dimethylaminopropyl) carbodiimide (EDC). After one hour of incubation, 2-mercaptoethanol (2-ME) (0.5 μL) was added to the reaction mixture to quench the unreacted EDC, then 50 mg (0.1 mmoles) of the carboxyl (CA) polyethylene glycol amino acids [CA$(PEG)_8$]) in 100 mmol PBS, pH 7.4, was added. The reaction mixture was left overnight with shaking, and then 50 μL of 25 mmol glycine was added to quench remaining activated sites on the particle surface. The resulting product was dialyzed against 2 L of the 10 mmol PBS, pH 7.4, for three hours.

A solution of the Fe_3O_4–DOPAC–$(PEG)_8$–COOH (150 μL) in PBS was mixed with 18.5 mg (80 μmoles) of sulfo-NHS and 3.2 mg (16.7 μmoles) of EDC dissolved in 15 μL of 100 mmol PBS, pH 6.3, and incubated for one hour with agitation. A total of 0.5 μL of 2-ME was added to quench unreacted EDC, and 400 μL of adenoviral (Ad) capsids in tris(hydroxymethyl)aminomethane (TRIS) buffer, pH 8, was added. The reaction mixture was left for three hours with gentle shaking, and then 20 μL of 25 mmol glycine was added. The resulting nanoparticle-labeled viral capsids were dialyzed overnight against 2 L of the 10 mmol PBS, pH 7.4 (Fig. 1). Unlabeled and SPION-labeled viral capsids were imaged using a Philips CM 30 transmission electron microscope (120 kV) (Amsterdam, The Netherlands).

2.2. Co-infusion of wild-type Ad5-GFP with rhodamine-dextran into rat brain

Osmotic pumps (Model 2ML1, ALZET, Cupertino, CA, USA) containing a solution of 2 mg rhodamine–dextran (Sigma-Aldrich) and 5.0×10^9 viral particles (vp) of wild-type Ad5-

green fluorescent protein (GFP) (Vector Biolabs; Philadelphia, PA, USA) were implanted into adult, male Harlan Sprague Dawley rats ($n = 3$). Infusion occurred for 96 hours at a rate of 10 μL/hour. The rats were then sacrificed and the brains were harvested and fixed. The brains were sectioned into 150 μm slices using a vibratome.

2.3. Ad5/3-cRGD-GFP transduction in U87 glioma cells and normal human astrocytes

U87 glioma cells and normal human astrocytes (NHA) were plated at 5.0×10^5 cells per well in a six-well plate and cultured in Dulbecco's Modified Eagle Medium with 10% fetal bovine serum (Invitrogen; Carlsbad, CA, USA) supplemented with sodium pyruvate and antibiotics. Virus was added to the wells at increasing concentrations (0, 1.0×10^4, 5.0×10^4, and 1.0×10^5 vp/cell) in triplicate. To evaluate the effect of labeling on vectors, U87 cells were infected with Ad5/3cRGD-GFP with or without nano-particle labeling at 1.0×10^2 vp/cell and compared to culture in free nanoparticles. Fluorescent microscopy (Nikon; Melville, NY, USA) and flow cytometry (BD Biosciences; Franklin Lakes, NJ, USA) were performed 48 hours post-infection. Statistics were performed using the one-way analysis of variance test using Prism version 5 (Graph-Pad Software; San Diego, CA, USA).

2.4. MRI detection of SPION-labeled Ad5/3-cRGD-GFP in a porcine model

An *in vivo* study of MRI detectability of SPION-labeled Ad5/3 cRGD-GFP was performed in a male pig. The infusate, which contained 1.0×10^9 labeled Ad5/3 cRGD–GFP particles in 0.5 mL saline, was infused into the prefrontal white matter at a rate of 0.017 mL/minute over 30 minutes to minimize back-leak. A contralateral infusion was performed with saline. Imaging occurred at 0, 24, 48, and 72 hours post-infusion on a 3-Tesla MRI, using T2-weighted (repetition time [TR] = 3000 ms, echo time [TE] = 80 ms) and gradient echo (GRE; TR = 1450 ms, TE = 16 ms) sequences. Manual volumetric analysis was then performed (OsiriX; Los Angeles, CA, USA). A necropsy was then performed and the brain was fixed. The sections were stained with hematoxylin and eosin (H&E) and immunohistochemical analysis was performed using anti-hexon antibody (1:500 dilution, ViroStat, Portland, ME, USA).

3. Results

3.1. Adenovirus and surrogate marker co-infusion results in different volumes of distribution

We co-infused rhodamine–dextran and wild-type Ad5-GFP into rat brains. Fluorescent analyses of the slices demonstrated that rhodamine–dextran penetrated distantly in the ipsilateral hemisphere and crossed the corpus callosum, whereas the GFP expression from adenovirus remained localized (Fig. 2).

3.2. Ad5/3-cRGD capsid modification results in preferential transduction of U87 cells

We found that following infection with Ad5/3-cRGD-GFP, greater GFP expression was seen in U87 cells compared to NHA at 5.0×10^4 vp/cell ($p < 0.0001$) (Fig. 3).

3.3. SPION-labeled Ad5/3-cRGD remains infective and is detectable in vivo by MRI

Electron microscopy of SPION-labeled adenovirus revealed specific and efficient labeling. No free nanoparticles or unlabeled capsids were observed (Fig. 4). Ad5/3 cRGD-GFP ± SPION demonstrated similar transduction efficiency, with all U87 cells expressing GFP post-infection. No fluorescence was observed with incubation in free SPION (Fig. 5).

Ferromagnetic particles act as T2 contrast agents.[29,30] *In vivo* detection of the nanoparticle-labeled vectors was demonstrated by comparing injection of SPION-labeled adenovirus to contralateral saline injection into prefrontal white matter of a porcine brain. A T2-weighted hyperintensity appeared on the virus-injected hemisphere, whereas saline produced no change. The gradient echo (GRE) sequence demonstrated a hypointensity at the virus injection site, which was present, but less so, on the contralateral hemisphere. These changes persisted up to 72 hours post-injection (Fig. 6A). There was stability of the T2 and GRE volumes (Fig. 6B).

Non-specific background was observed with immunostaining using anti-hexon antibody, likely due to cross-reactivity to the pig tissue. Staining with H&E demonstrated tract hemorrhages bilaterally (data not shown).

4. Discussion

Virus-mediated gene therapy is a promising modality for the treatment of malignant gliomas. However, volumes of distribution are limiting factors.[6] Methods exist, such as convection-enhanced delivery, which allow for better distribution of vectors and macro-molecules. [31] To evaluate these methods, vectors need to be tracked precisely. Previous studies have described distribution through coinfusion of analogs, which is not the optimal method to describe volumes, as the distribution by convection is determined by size, concentration, affinity, and non-covalent interactions.[32–34] We demonstrate this through the co-infusion of Ad5-GFP and rhodamine–dextran, which achieved different volumes as the dextran reached the contralateral hemisphere. Hence, co-infusion of a marker cannot accurately estimate the volume of distribution of a viral vector, as explained by Chen et al., who concluded that surface properties influence the distribution of viral particles.[34]

Capsid modifications can increase glioma tropism. We describe a novel Ad5/3-cRGD that exhibits tropism towards receptors highly expressed by glioma cells.[15] We confirmed the concentration-dependent transduction ability of Ad5/3-cRGD-GFP in U87. Further, SPION-labeled capsids retain their ability to transduce glioma cells.

MRI detectability of SPION-labeled virus was assessed by injection into a porcine brain. T2-weighted hyperintensity was shown with SPION-labeled virus injection corresponding with GRE hypointensity, which were not present with saline injection. These changes persisted until 72 hours post-injection. We acknowledge that the SPION-labeling process may affect surface properties of the capsid, which could affect the volume of distribution.

Imaging in gene therapy is key for improving of volumes of distribution and localization of its effects. Traditionally, vectors have been tracked based upon gene transduction or biodistribution, using single photon emission tomography and positron emission tomography to assess gene delivery.[35,36] The use of MRI has been limited by poor detection of vectors without exogenous contrast agent administration; therefore, co-infusion of vectors with virus-sized nanoparticles was utilized to attempt to determine effective distribution.[21] However, as described above, surface properties, more so than size, affect volumes of distribution.[35] In this study, we demonstrate the development of a vector that functions as a contrast agent to increase the specificity of MRI detection and present the first study, to our knowledge, to describe *in vivo* imaging characteristics following injection into a large brain model.

Acknowledgments

This work was supported in part by the Alpha Omega Alpha Carolyn L. Kuckein Research Fellowship (JY). Work at Argonne, including the use of the Center for Nanoscale Materials, was supported by the U. S. Department of Energy, Office of Science, Office of Basic Energy Sciences, under Contract No. DE-AC02-06CH11357. Dr. Lesniak's research was supported by a grant from NIH/NINDS R01NS077388.

References

1. Stupp R, Mason WP, van den Bent MJ, et al. Radiotherapy plus concomitant and adjuvant temozolomide for glioblastoma. N Engl J Med. 2005; 352:987–96. [PubMed: 15758009]
2. Verhaak RG, Hoadley KA, Purdom E, et al. Integrated genomic analysis identifies clinically relevant subtypes of glioblastoma characterized by abnormalities in PDGFRA, IDH1, EGFR, and NF1. Cancer Cell. 2010; 17:98–110. [PubMed: 20129251]
3. Trask TW, Trask RP, Aguilar-Cordova E, et al. Phase I study of adenoviral delivery of the HSV-tk gene and ganciclovir administration in patients with current malignant brain tumors. Mol Ther. 2000; 1:195–203. [PubMed: 10933931]
4. Sandmair AM, Loimas S, Puranen P, et al. Thymidine kinase gene therapy for human malignant glioma, using replication-deficient retroviruses or adenoviruses. Hum Gene Ther. 2000; 11:2197–205. [PubMed: 11084677]
5. Germano IM, Fable J, Gultekin SH, et al. Adenovirus/herpes simplex-thymidine kinase/ganciclovir complex: preliminary results of a phase I trial in patients with recurrent malignant gliomas. J Neurooncol. 2003; 65:279–89. [PubMed: 14682378]
6. Lang FF, Bruner JM, Fuller GN, et al. Phase I trial of adenovirus-mediated p53 gene therapy for recurrent glioma: biological and clinical results. J Clin Oncol. 2003; 21:2508–18. [PubMed: 12839017]
7. Fuxe J, Liu L, Malin S, et al. Expression of the coxsackie and adenovirus receptor in human astrocytic tumors and xenografts. Int J Cancer. 2003; 103:723–9. [PubMed: 12516090]
8. Li D, Duan L, Freimuth P, et al. Variability of adenovirus receptor density influences gene transfer efficiency and therapeutic response in head and neck cancer. Clin Cancer Res. 1999; 5:4175–81. [PubMed: 10632357]
9. Sonabend AM, Ulasov IV, Lesniak MS. Conditionally replicative adenoviral vectors for malignant glioma. Rev Med Virol. 2006; 16:99–115. [PubMed: 16416455]
10. Mercer RW, Tyler MA, Ulasov IV, et al. Targeted therapies for malignant glioma: progress and potential. BioDrugs. 2009; 23:25–35. [PubMed: 19344189]
11. Paul CP, Everts M, Glasgow JN, et al. Characterization of infectivity of kno-modified adenoviral vectors in glioma. Cancer Biol Ther. 2008; 7:786–93. [PubMed: 18756624]
12. Tyler MA, Ulasov IV, Borovjagin A, et al. Enhanced transduction of malignant glioma with a double targeted Ad5/3-RGD fiber-modified adenovirus. Mol Cancer Ther. 2006; 5:2408–16. [PubMed: 16985075]
13. Ulasov IV, Rivera AA, Han Y, et al. Targeting adenovirus to CD80 and CD86 receptors increases gene transfer efficiency to malignant glioma cells. J Neurosurg. 2007; 107:617–27. [PubMed: 17886563]
14. Ulasov IV, Tyler MA, Han Y, et al. Novel recombinant adenoviral vector that targets the interleukin-13 receptor alpha2 chain permits effective gene transfer to malignant glioma. Hum Gene Ther. 2007; 18:118–29. [PubMed: 17328684]
15. Zheng S, Ulasov IV, Han Y, et al. Fiber-knob modifications enhance adenoviral tropism and gene transfer in malignant glioma. J Gene Med. 2007; 9:151–60. [PubMed: 17351980]
16. Steck PA, Moser RP, Bruner JM, et al. Altered expression and distribution of heparan sulfate proteoglycans in human gliomas. Cancer Res. 1989; 49:2096–103. [PubMed: 2522816]
17. Maenpaa A, Junnikkala S, Hakulinen J, et al. Expression of complement membrane regulators membrane cofactor protein (CD46), decay accelerating factor (CD55), and protectin (CD59) in human malignant gliomas. Am J Pathol. 1996; 148:1139–52. [PubMed: 8644856]
18. Barker FG 2nd, Chang SM, Gutin PH, et al. Survival and functional status after resection of recurrent glioblastoma multiforme. Neurosurgery. 1998; 42:709–20. discussion 20–3. [PubMed: 9574634]
19. Lopez KA, Waziri AE, Canoll PD, et al. Convection-enhanced delivery in the treatment of malignant glioma. Neurol Res. 2006; 28:542–8. [PubMed: 16808887]
20. Fiandaca MS, Varenika V, Eberling J, et al. Real-time MR imaging of adenoassociated viral vector delivery to the primate brain. Neuroimage. 2009; 47:T27–35. [PubMed: 19095069]

21. Szerlip NJ, Walbridge S, Yang L, et al. Real-time imaging of convection-enhanced delivery of viruses and virus-sized particles. J Neurosurg. 2007; 107:560–7. [PubMed: 17886556]
22. Su X, Kells AP, Aguilar Salegio EA, et al. Real-time MR imaging with gadoteridol predicts distribution of transgenes after convection-enhanced delivery of AAV2 vectors. Mol Ther. 2010; 18:1490–5. [PubMed: 20551915]
23. Laurent S, Bridot JL, Elst LV, et al. Magnetic iron oxide nanoparticles for biomedical applications. Future Med Chem. 2010; 2:427–49. [PubMed: 21426176]
24. Mahmoudi M, Hosseinkhani H, Hosseinkhani M, et al. Magnetic resonance imaging tracking of stem cells in vivo using iron oxide nanoparticles as a tool for the advancement of clinical regenerative medicine. Chem Rev. 2011; 111:253–80. [PubMed: 21077606]
25. Antonelli A, Sfara C, Manuali E, et al. Encapsulation of superparamagnetic nanoparticles into red blood cells as new carriers of MRI contrast agents. Nanomedicine (Lond). 2011; 6:211–23. [PubMed: 21385124]
26. Yallapu MM, Othman SF, Curtis ET, et al. Multi-functional magnetic nanoparticles for magnetic resonance imaging and cancer therapy. Biomaterials. 2011; 32:1890–905. [PubMed: 21167595]
27. Huh YM, Lee ES, Lee JH, et al. Hybrid nanoparticles for magnetic resonance imaging of target-specific viral gene delivery. Adv Mater. 2007; 19:3109–12.
28. Sun S, Zeng H, Robinson DB, et al. Monodisperse MFe_2O_4 (M = Fe, Co, Mn) nanoparticles. J Am Chem Soc. 2004; 126:273–9. [PubMed: 14709092]
29. Yang H, Zhuang Y, Sun Y, et al. Targeted dual-contrast T(1)- and T(2)-weighted magnetic resonance imaging of tumors using multifunctional gadoliniumlabeled superparamagnetic iron oxide nanoparticles. Biomaterials. 2011; 32:4584–93. [PubMed: 21458063]
30. Raty JK, Liimatainen T, Unelma Kaikkonen M, et al. Non-invasive imaging in gene therapy. Mol Ther. 2007; 15:1579–86. [PubMed: 17579578]
31. Bobo RH, Laske DW, Akbasak A, et al. Convection-enhanced delivery of macromolecules in the brain. Proc Natl Acad Sci U S A. 1994; 91:2076–80. [PubMed: 8134351]
32. Kroll RA, Pagel MA, Muldoon LL, et al. Increasing volume of distribution to the brain with interstitial infusion: dose, rather than convection, might be the most important factor. Neurosurgery. 1996; 38:746–52. [PubMed: 8692395]
33. Chen MY, Lonser RR, Morrison PF, et al. Variables affecting convection-enhanced delivery to the striatum: a systematic examination of rate of infusion, cannula size, infusate concentration, and tissue-cannula sealing time. J Neurosurg. 1999; 90:315–20. [PubMed: 9950503]
34. Chen MY, Hoffer A, Morrison PF, et al. Surface properties, more than size, limiting convective distribution of virus-sized particles and viruses in the central nervous system. J Neurosurg. 2005; 103:311–9. [PubMed: 16175862]
35. Li GC, He F, Ling CC. Hyperthermia and gene therapy: potential use of microPET imaging. Int J Hyperthermia. 2006; 22:215–21. [PubMed: 16754341]
36. Penuelas I, Boan J, Marti-Climent JM, et al. Positron emission tomography and gene therapy: basic concepts and experimental approaches for in vivo gene expression imaging. Mol Imaging Biol. 2004; 6:225–38. [PubMed: 15262238]

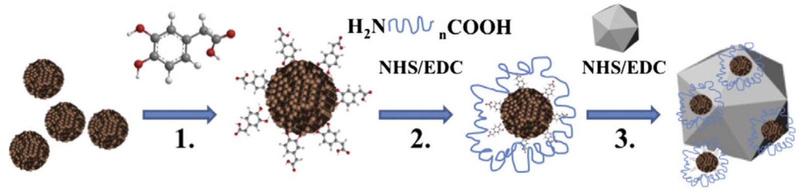

Fig. 1.

Schematic of the synthesis of nanoparticle (NP)-labeled adenoviral capsids. **1**. NP (10 nm) were transferred to the water phase through ligand exchange via chemisorption of catecholate ligand (3,4-dihydroxyphenylacetic acid [DOPAC]) on the NP surface. **2**. DOPAC was then functionalized with bi-functional carboxyl- (polyethylene glycol)$_8$-amine (CA[PEG]$_8$) using carbodiimide coupling chemistry. **3**. Resulting NP functionalized with PEG$_8$ brushes were linked to the adenoviral capsids as described in Section 2.1 of this article. EDC = 1-ethyl-3-(3-dimethylaminopropyl) carbodiimide, NHS = sulfo-N-hydroxysuccinimide.

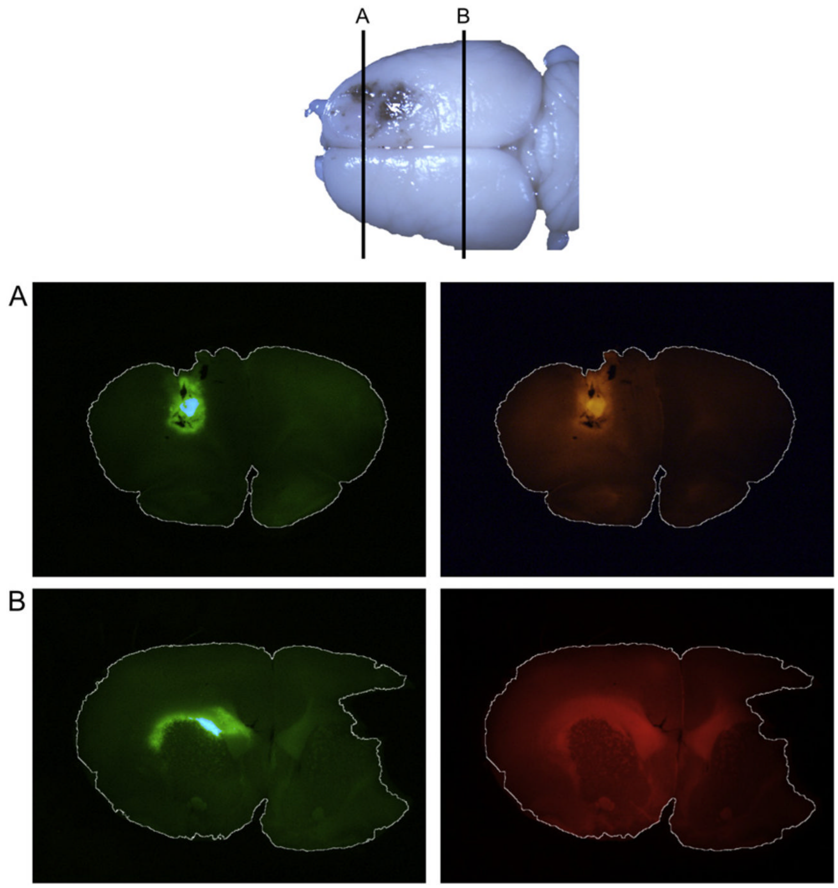

Fig. 2.

Ad5-green fluorescent protein (GFP) and rhodamine–dextran distribution in coronal rat brain slices. Ad5-GFP and rhodamine–dextran were co-infused intracranially in male rats. (A) GFP (green) expression is highest around the site of injection and rhodamine–dextran (red) is seen throughout the hemisphere. (B) At a more caudal slice, rhodamine–dextran shows greater spread across the corpus callosum. A smaller area of GFP expression is confined to the white matter.

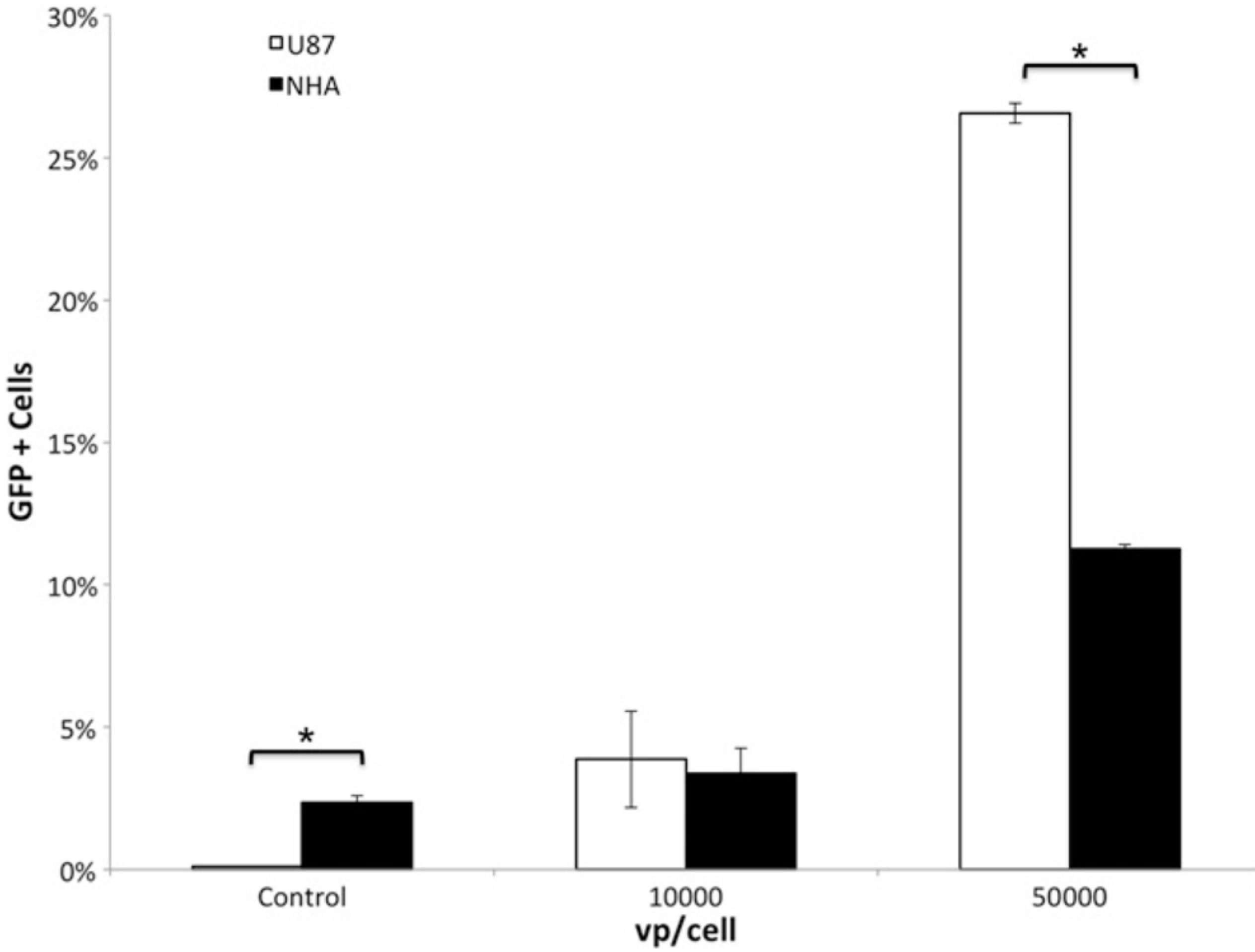

Fig. 3.

Histogram of flow cytometry of green fluorescent protein (GFP) expression with adenoviral capsid (Ad5/3-cRGD). Infection of U87 glioma cell line and normal human astrocytes (NHA) with Ad5/3-cRGD showed a significantly higher percentage of GFP+ cells in U87 compared to NHA at 5.0×10^4 viral particles (vp)/cell.

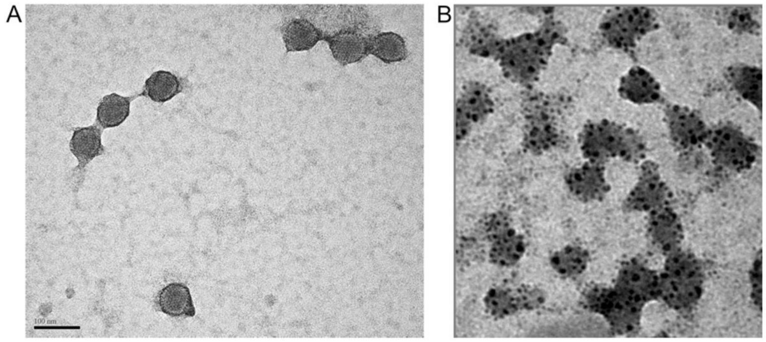

Fig. 4.
Transmission electron microscopy of unlabeled (A) and super-paramagnetic iron oxide (Fe_3O_4) nanoparticles (SPION)-labeled (B) adenoviral capsid (Ad5/3 cRGD). For the SPION-labeled Ad5/3 cRGD there are no unlabeled capsids and/or free particles remaining. Bar represents 100 nm.

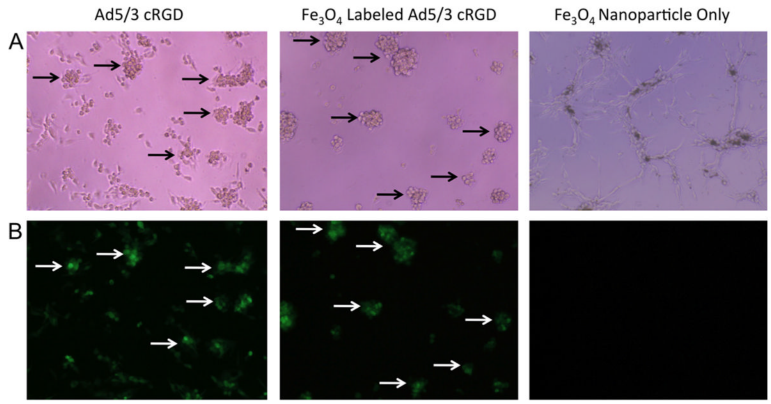

Fig. 5.

U87 cells cultured with super-paramagnetic iron oxide (Fe_3O_4) nanoparticles (SPION) unlabeled and labeled adenoviral capsid (Ad5/3 cRGD-GFP) and free nanoparticles. Plates viewed under (A) light (hematoxylin and eosin, ×20) and (B) fluorescent microscopy for green fluorescent protein (GFP) (×20) demonstrate that unlabeled Ad5/3 cRGD effectively transduces U87 glioma cells, with all clusters expressing GFP. SPION-labeled Ad5/3 cRGD demonstrates equivalent efficiency. No GFP+ cells are seen with free nanoparticles.

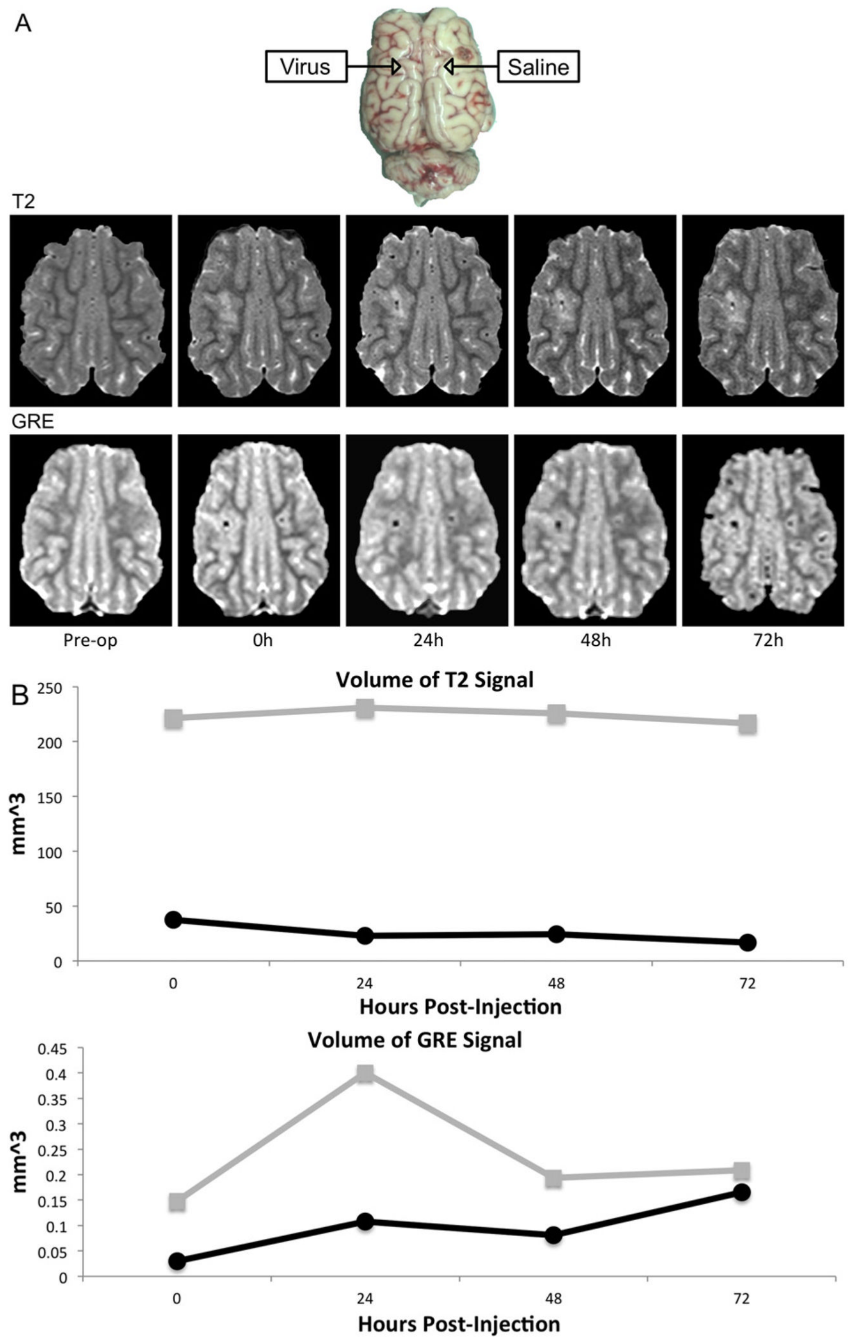

Fig. 6.

Post-injection imaging of super-paramagnetic iron oxide (Fe_3O_4) nanoparticle (SPION)-Ad5/3 cRGD and saline. Nanoparticle-labeled Ad5/3-cRGD-green fluorescent protein (GFP) was injected into subcortical white matter of a pig and contralateral saline injection was used as a control. (A) Axial (upper) T2-weighted MRI showing greater T2-weighted hyperintense area around the site of virus compared to saline injection that persists for up to 72 hours; and (lower) gradient echo (GRE) showing hypointensity at the virus site, and a smaller area of hypointensity on the saline-infused side. (B) The volume of T2 hyperintensity is greater with virus injection (gray) compared to saline injection (black) as measured by both T2-weighted and GRE signal.